

Sparse MeZO: Less Parameters for Better Performance in Zeroth-Order LLM Fine-Tuning

Yong Liu¹ Zirui Zhu¹ Chaoyu Gong¹ Minhao Cheng² Cho-Jui Hsieh³ Yang You¹

Abstract

While fine-tuning large language models (LLMs) for specific tasks often yields impressive results, it comes at the cost of memory inefficiency due to back-propagation in gradient-based training. Memory-efficient Zeroth-order (MeZO) optimizers, recently proposed to address this issue, only require forward passes during training, making them more memory-friendly. However, the quality of gradient estimates in zeroth order optimization often depends on the data dimensionality, potentially explaining why MeZO still exhibits significant performance drops compared to standard fine-tuning across various tasks. Inspired by the success of Parameter-Efficient Fine-Tuning (PEFT), this paper introduces Sparse MeZO, a novel memory-efficient zeroth-order optimization approach that applies ZO only to a carefully chosen subset of parameters. We propose a simple yet effective parameter selection scheme that yields significant performance gains with Sparse-MeZO. Additionally, we develop a memory-optimized implementation for sparse masking, ensuring the algorithm requires only inference-level memory consumption, allowing Sparse-MeZO to fine-tune LLaMA-30b on a single A100 GPU. Experimental results illustrate that Sparse-MeZO consistently improves both performance and convergence speed over MeZO without any overhead. For example, it achieves a 9% absolute accuracy improvement and 3.5x speedup over MeZO on the RTE task.

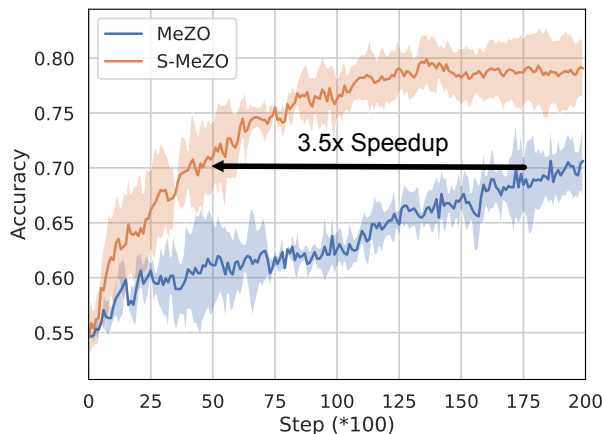


Figure 1. Performance of MeZO and Sparse-MeZO (S-MeZO) on RTE task. S-MeZO can achieve 3.5x speedup compared with MeZO.

1. Introduction

Fine-tuning large language models for specific tasks or datasets has become a prevalent practice in machine learning. However, a major obstacle in fine-tuning is the substantial memory requirements, which escalate as models increase in size and complexity, thereby limiting the scalability and accessibility for those with limited computational resources.

To mitigate the memory constraints, Parameter Efficient Fine-Tuning (PEFT) has been developed, allowing for the modification of only a subset of parameters and achieving comparable results to full model tuning (Zaken et al., 2021; Li & Liang, 2021; Lester et al., 2021; Hu et al., 2021; Zhang et al., 2023). However, PEFT methods still necessitate the calculation of gradients for backpropagation and caching of numerous activations during training, which introduces additional memory overhead. For instance, Malladi et al. demonstrates that, even with PEFT, training still requires approximately 6 times more memory than the memory cost for inference. This discrepancy raises a critical question: Can large language models be fine-tuned solely with the cost of inference?

In response to these challenges, zeroth-order (ZO) optimization presents a promising solution (Spall, 1992). ZO

¹Department of Computer Science, National University of Singapore, Singapore ²College of Information Sciences and Technology, Penn State University, USA ³Department of Computer Science, University of California, Los Angeles, USA. Correspondence to: Yong Liu <liuyong@comp.nus.edu.sg>, Yang You <youy@comp.nus.edu.sg>.

optimization is a gradient-free method that estimates gradients using only the forward pass of the model, eliminating the need for backpropagation and, consequently, reducing memory usage. MeZO (Malladi et al., 2023) is a recently proposed zeroth-order method for fine-tuning LLMs that has demonstrated impressive performance. However, the performance and convergence rate of ZO methods are usually highly dependent on the dimensionality of the parameters, with higher dimensionality leading to slower convergence.

Building on the insights from PEFT, we propose a novel sparse memory efficient zeroth-order method (Sparse-MeZO) to solve the issues from the high dimensionality of LLMs. In traditional parameter-efficient fine-tuning, there’s a tradeoff between memory efficiency and performance. But surprisingly, when we only tune a subset of parameters in MeZO, it significantly improves the performance while accelerating the convergence rate. This renders our method an improvement over MeZO without any overhead. Our contributions can be summarized as follows:

- In this paper, we propose a sparse Memory-Efficient Zeroth-Order optimization method Sparse-MeZO (S-MeZO) for large language model fine-tuning. We also provide theoretical analysis to show the convergence of Sparse-MeZO.
- To determine the sparse parameters that need to be updated, we investigate how the importance of each parameter in fine-tuning correlates with its magnitude. Although existing sparsification methods usually prune out parameters with smaller magnitudes, our evaluations show that smaller parameters are more important than larger weights for Zeroth-order fine-tuning methods.
- Different from the efficient implementation with random seed in MeZO, we propose a novel memory-efficient implementation of Sparse-MeZO, which can compute the sparse mask and perturb parameters in the forward pass. The technique enables fine-tuning LLaMA-30b with Sparse-MeZO on a single A100 GPU.
- We conduct empirical studies on LLaMA and OPT. The experimental results demonstrate that Sparse-MeZO can improve the fine-tuning performance and yield a faster convergence rate compared with vanilla MeZO across a wide range of natural language processing tasks. For example, it achieves a 9% absolute accuracy improvement and 3.5x speedup over MeZO on the RTE task, as shown in Figure 1.

2. Preliminaries

2.1. Parameter-Efficient Fine-Tuning

Parameter-Efficient Fine-Tuning (PEFT) is designed to facilitate efficient adaptation by updating only a subset of

the model’s parameters, rather than fine-tuning the entire model (Hu et al., 2021; Zaken et al., 2021). These PEFT approaches can be categorized in various ways. We mainly focus on the selective methods and additive methods.

2.1.1. SELECTIVE METHODS

Selective Methods try to selectively fine-tune a portion of a model and these methods have been explored in various studies. For example, Zaken et al.; Cai et al. focused on the model’s bias terms, finding that fine-tuning these terms alone could rival the results of fine-tuning the entire model. However, the effectiveness of this approach diminishes with larger datasets, as shown in further analysis by Zaken et al.. Beyond static parameter adjustments, there has been an exploration into dynamically modifying parts of the model. For instance, FreezeOut, introduced by Brock et al., suggests a gradual freezing of layers, effectively removing early layers from the backward pass to quicken training. This concept was later applied to language models, with AutoFreeze (Liu et al., 2021) confirming its viability. Nevertheless, these techniques still demand considerable computational resources and tend to yield less optimal final outcomes.

2.1.2. ADDITIVE METHODS

Additive methods, as an alternative to updating existing parameters, involve incorporating new layers into models, with the fine-tuning process focusing solely on these added layers (Houlsby et al., 2019; Rebuffi et al., 2017; Lin et al., 2020; Hu et al., 2021). Traditional techniques in this category, such as adapters (Houlsby et al., 2019), implemented layer additions in a sequential manner, which unfortunately led to increased inference latency. LoRA (Hu et al., 2021) has been proposed to mitigate this issue, which freezes the weights of the pre-trained model and introduces trainable matrices based on rank decomposition into each layer. Then, it can directly integrate the newly learned weights into the main model. Following this, IA3 (Liu et al., 2022) introduced innovative methods for adding parameters, balancing parameter count with accuracy, while LST (Sung et al., 2022) introduced a highway structure that learns only small, auxiliary channels, aiming to decrease memory demands. Despite these advancements, additive methods generally require meticulous design, and many fail to reduce the computational load during the backward pass, as seen in IA3, LoRA, and Adapter approaches. Additionally, some of these methods, including Adapter and LST, can incur additional computational overhead in the forward pass, making them less practical for certain applications.

2.2. Zeroth-Order Optimization

Unlike traditional gradient-based optimization methods that rely on derivatives to guide the search for optimal solutions,

zeroth-order (ZO) optimization techniques do not require derivatives for optimization (Spall, 1992; Liu et al., 2018; 2019). These methods utilize only the value of the objective function, denoted as $f(\mathbf{x})$, at any chosen point \mathbf{x} . To estimate the gradient in the direction of vector \mathbf{z} , the objective function is assessed at two points in close proximity, $f(\mathbf{x} + \epsilon\mathbf{z})$ and $f(\mathbf{x} - \epsilon\mathbf{z})$, with ϵ being a minimal value. Following this, conventional optimization algorithms, such as gradient descent or coordinate descent, are implemented using these approximated gradient values. Currently, ZO methods have been widely used in various applications, such as adversarial attack and defense (Chen et al., 2017; Tu et al., 2019; Ye et al., 2018; Ilyas et al., 2018), Auto-ML (Ruan et al., 2019; Wang et al., 2022), natural language processing (Sun et al., 2022a;b), reinforcement learning (Vemula et al., 2019), Signal Processing (Liu et al., 2020), and on-chip training (Gu et al., 2021).

2.2.1. SPSA

Simultaneous Perturbation Stochastic Approximation (SPSA) (Spall, 1992) is a descent method that optimizes systems with multiple unknown parameters to identify global minima without relying on backpropagation. SPSA estimates gradients based on two measurements of the objective function, thus eliminating the need for automatic differentiation and backpropagation to obtain precise gradients. This approach notably avoids memory overhead associated with storing intermediate results for backpropagation. Specially, it employs a random vector $\mathbf{z} \in \mathbb{R}^d$, where $\mathbf{z} \sim \mathcal{N}(\mathbf{0}, \mathcal{I}_d)$, to define to perturb the parameters and estimate the gradient based on the difference between $\mathcal{L}(\boldsymbol{\theta} + \epsilon\mathbf{z})$ and $\mathcal{L}(\boldsymbol{\theta} - \epsilon\mathbf{z})$:

$$\begin{aligned} \mathbf{g}_{\mathbf{z}}(\boldsymbol{\theta}) &= \frac{\mathcal{L}(\boldsymbol{\theta} + \epsilon\mathbf{z}) - \mathcal{L}(\boldsymbol{\theta} - \epsilon\mathbf{z})}{2\epsilon} \mathbf{z} \\ &\approx \mathbf{z}\mathbf{z}^\top \mathbf{g}(\boldsymbol{\theta}). \end{aligned} \quad (1)$$

2.2.2. MeZO

ZO-SGD employs SPSA to estimate the gradient. In general, conventional ZO-SGD algorithms utilizing SPSA consume twice the inference memory. MeZO (Malladi et al., 2023) is a memory-efficient variant of ZO-SGD. It circumvents the storage of gradients by saving the random seed and resampling the same random noise \mathbf{z} with the seed during forward process. Therefore, it can reduce the training costs close to inference memory cost.

We try to further explain how MeZO can be memory-efficient in Figure 2. At step 1, it will sample a noise \mathbf{z} to perturb $\boldsymbol{\theta}_t$ and then can obtain $\boldsymbol{\theta}'_t$ to calculate \mathcal{L}^+ . At step 2, MeZO can resample the same noise \mathbf{z} with same seed s_t to directly perturb $\boldsymbol{\theta}'_t$ but not $\boldsymbol{\theta}_t$. Then, it can use $\boldsymbol{\theta}'_t - 2\epsilon\mathbf{z}$ to reconstruct $\boldsymbol{\theta}_t - \epsilon\mathbf{z} = \boldsymbol{\theta}''_t$ without additional memory cost and finally calculate the loss value \mathcal{L}^- .

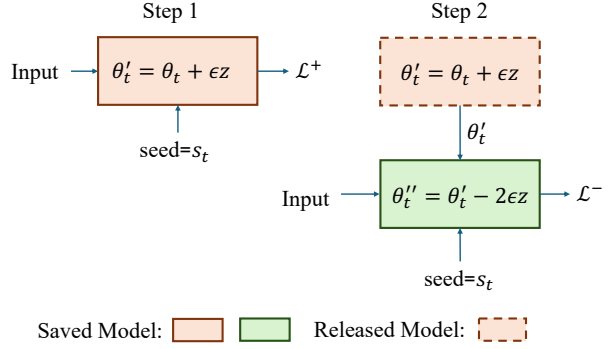


Figure 2. Memory Efficient Implementation in MeZO. At step 1, we will sample a random noise \mathbf{z} to perturb $\boldsymbol{\theta}'_t = \boldsymbol{\theta}_t + \epsilon\mathbf{z}$ and save the seed s_t . At step 2, MeZO can resample the same noise \mathbf{z} with same s_t to calculate $\boldsymbol{\theta}''_t = \boldsymbol{\theta}'_t - 2\epsilon\mathbf{z} = \boldsymbol{\theta}_t - \epsilon\mathbf{z}$ and release the memory of $\boldsymbol{\theta}'_t$.

2.2.3. SPARSITY FOR ZEROth-ORDER OPTIMIZATION

The hypothesis proposed by Frankle & Carbin, known as the lottery ticket hypothesis, showed that within a densely connected neural network that is randomly initialized, there exists a subnetwork of sparse yet high-quality connections. Several related works have tried to apply the sparsity to zeroth-order optimization (Wang et al., 2018; Cai et al., 2022; 2021; Balasubramanian & Ghadimi, 2018; Ohta et al., 2020; Gu et al., 2021; Chen et al., 2023). For example, DeepZero proposes a novel ZO training protocol with model pruning guided sparsity. However, these methods mainly focus on the neural network training from scratch with random initialization, while the application of sparse zeroth-order optimization in fine-tuning tasks remains an area of ongoing exploration. In this paper, we will analyze the effects of sparse ZO methods on large language model fine-tuning tasks and propose a novel sparse zeroth-order method to obtain a better performance and faster convergence.

3. Proposed Method

Parameter-Efficient Fine-Tuning (PEFT) has been widely used in various areas, which only updates a fraction of full parameters and can yield comparable performance. In addition, it's widely recognized that both the performance and the convergence rate are significantly influenced by the dimensionality of the weights to ZO methods. For example, Duchi et al. illustrates that an increase in dimensionality tends to proportionally slow down the convergence rate. These motivate us to propose a sparse zeroth-order optimization method for large language model fine-tuning, which only updates a subset of full parameters and yields a comparable performance and faster convergence.

3.1. Sparse-MeZO

Consider a labelled dataset $\mathcal{D} = \{(\mathbf{x}_i, \mathbf{y}_i)\}_{i \in [|\mathcal{D}|]}$ and let $\mathcal{L}(\theta; \mathcal{B})$ denotes the loss on a mini-batch \mathcal{B} . We can define a sparse mask $\mathbf{m} \in \{0, 1\}^d$ to selectively sample the random noise $\mathbf{z} \in \mathbb{R}^d$ with $\mathbf{z} \sim \mathcal{N}(\mathbf{0}, \mathbf{I}_d)$ on the sub-net of pre-trained model. A sparsified version of random perturbation can be defined as $\hat{\mathbf{z}} \in \mathbb{R}^d$:

$$\hat{\mathbf{z}} = \mathbf{m} \odot \mathbf{z}. \quad (2)$$

Based on this sparse perturbation $\hat{\mathbf{z}}$, we can redefine MeZO algorithm on Section 2.2.2 as Sparse-MeZO. The main difference is from the estimated gradient $\mathbf{g}_{\hat{\mathbf{z}}}(\theta)$, which can be defined as :

$$\begin{aligned} \mathbf{g}_{\hat{\mathbf{z}}}(\theta) &= \frac{\mathcal{L}(\theta + \epsilon \hat{\mathbf{z}}; \mathcal{B}) - \mathcal{L}(\theta - \epsilon \hat{\mathbf{z}}; \mathcal{B})}{2\epsilon} \\ &= \frac{\mathcal{L}(\theta + \epsilon \mathbf{m} \odot \mathbf{z}; \mathcal{B}) - \mathcal{L}(\theta - \epsilon \mathbf{m} \odot \mathbf{z}; \mathcal{B})}{2\epsilon}, \end{aligned} \quad (3)$$

where ϵ represents the perturbation scale. Note that although working with a sparse perturbation, we still need to use full parameters θ in the forward process to calculate the loss value $\mathcal{L}(\theta + \epsilon \hat{\mathbf{z}})$.

3.2. Convergence Analysis of Sparse-MeZO

In this section, we will explain why Sparse-MeZO can accelerate the convergence. We can define a sub-network in pre-trained large language models, which is determined by the sparse mask \mathbf{m} . The main idea of our proof is that if we follow the updated role in Sparse-MeZO, the gradient norm on the sub-network can be smaller than σ^2 after $\mathcal{O}(\frac{\hat{d}L}{\sigma^2})$ steps, where \hat{d} is the number of parameters in the sub-network. Therefore, ZO can use fewer steps to converge when we only focus on a sub-network. Some related work has illustrated that only tuning the sub-network can achieve comparable performance, which will be empirically verified in our experiments.

Firstly, we assume the loss function $\mathcal{L}(\theta; \mathbf{x})$ is Lipschitz Continuous:

Assumption 3.1 (Lipschitz Continuous).

$$\|\nabla \mathcal{L}(\theta; \mathbf{x}) - \nabla \mathcal{L}(\theta'; \mathbf{x})\| \leq \frac{L(l)}{2} \|\theta - \theta'\|^2, \quad (4)$$

where $\nabla \mathcal{L}(\theta; \mathbf{x})$ denotes the true first-order gradient of θ on \mathbf{x} and $L(l)$ represents the Lipschitz constant of $\mathcal{L}(\cdot)$. Given $\mathcal{L}_{\hat{\mathbf{z}}}(\theta) = \mathbb{E}_{\hat{\mathbf{z}}}[\mathcal{L}(\theta + \epsilon \hat{\mathbf{z}})]$ and the above Assumption 3.1, we can obtain the relationship between sparse gradient $\hat{\nabla}_{\theta} \mathcal{L}_{\hat{\mathbf{z}}}(\theta)$ and the expectation of estimated sparse ZO gradient $\mathbf{g}_{\hat{\mathbf{z}}}(\theta)$:

Lemma 3.2. ZO gradient $\mathbf{g}_{\hat{\mathbf{z}}}(\theta)$ is unbiased estimation of $\hat{\nabla}_{\theta} \mathcal{L}_{\hat{\mathbf{z}}}(\theta)$:

$$\begin{aligned} \hat{\nabla}_{\theta} \mathcal{L}_{\hat{\mathbf{z}}}(\theta) &= \mathbf{m} \odot \nabla_{\theta} \mathcal{L}_{\hat{\mathbf{z}}}(\theta) \\ &= \mathbf{m} \odot \nabla_{\theta} \mathbb{E}_{\hat{\mathbf{z}}}[\mathcal{L}(\theta + \epsilon \hat{\mathbf{z}})] \\ &= \mathbb{E}_{\hat{\mathbf{z}}}\left[\frac{\mathcal{L}(\theta + \epsilon \hat{\mathbf{z}}) - \mathcal{L}(\theta - \epsilon \hat{\mathbf{z}})}{2\epsilon} \hat{\mathbf{z}}\right] \\ &= \mathbb{E}_{\hat{\mathbf{z}}}[\mathbf{g}_{\hat{\mathbf{z}}}(\theta)], \end{aligned} \quad (5)$$

where $\mathbf{g}_{\hat{\mathbf{z}}}(\theta) = \frac{\mathcal{L}(\theta + \epsilon \hat{\mathbf{z}}) - \mathcal{L}(\theta - \epsilon \hat{\mathbf{z}})}{2\epsilon} \hat{\mathbf{z}}$. We can find that $\mathbf{g}_{\hat{\mathbf{z}}}(\theta)$ is unbiased estimation of $\hat{\nabla}_{\theta} \mathcal{L}_{\hat{\mathbf{z}}}(\theta)$. Then, based on the equation $\hat{\nabla}_{\theta} \mathcal{L}_{\hat{\mathbf{z}}}(\theta) = \mathbb{E}_{\hat{\mathbf{z}}}[\mathbf{g}_{\hat{\mathbf{z}}}(\theta)]$ in Lemma 3.2, we can use the distance $\|\hat{\nabla}_{\theta} \mathcal{L}_{\hat{\mathbf{z}}}(\theta) - \nabla_{\theta} \mathcal{L}_m(\theta)\|$ to analyze the relationship between the true sparse gradient $\nabla_{\theta} \mathcal{L}_m(\theta) = \mathbf{m} \odot \nabla_{\theta} \mathcal{L}(\theta)$ and sparse gradient $\hat{\nabla}_{\theta} \mathcal{L}_{\hat{\mathbf{z}}}(\theta)$:

Lemma 3.3. Let \mathcal{L} be Lipschitz Continuous, we have:

$$\|\nabla_{\theta} \mathcal{L}_m(\theta)\|^2 \leq 2\|\hat{\nabla}_{\theta} \mathcal{L}_{\hat{\mathbf{z}}}(\theta)\|^2 + \frac{\epsilon^2 L^2(l)}{2} (\hat{d} + 4)^3. \quad (6)$$

where $\nabla_{\theta} \mathcal{L}_m(\theta) = \mathbf{m} \odot \nabla_{\theta} \mathcal{L}(\theta)$, $\hat{d} = \sum_{i=1}^d m_i$ is the number of selected parameters in mask \mathbf{m} , $L(l)$ represents the Lipschitz constant. Finally, we can obtain the convergence rate of Sparse-MeZO.

Theorem 3.4. Assuming a sequence of generated parameters $\{\theta_t\}_{t \geq 0}$ in Sparse-MeZO. We can have:

$$\mathbb{E}_{\hat{\mathbf{z}}, x}[\|\nabla_{\theta} \mathcal{L}_m(\theta_T)\|^2] \leq \sigma^2 \quad (7)$$

for any $T = \mathcal{O}(\frac{\hat{d}L}{\sigma^2})$

where $L(l) \leq L$ for all $\mathcal{L}(\theta_t)$. This theorem illustrates that the presence of pronounced sparsity patterns, along with the smoothness of the objective function, can significantly enhance the rate of convergence, potentially achieving a linear acceleration.

3.3. Less Parameters for Better Performance

From the analysis above, we find that Sparse-MeZO can speed up the convergence of zeroth-order optimization. After that, the main problem is how to determine the sparse mask \mathbf{m} . Network pruning is a popular method to prune the unimportant parameters and only use these selected important parameters to make the inference process fast and efficient (LeCun et al., 1989; Hanson & Pratt, 1988; Hassibi & Stork, 1992; Ström, 1997; Han et al., 2015a;b). Specifically, it typically removes connections with small parameters and retains those with large values. Drawing from these recent studies in network pruning, we first explore how the value of parameters affects zeroth-order optimization. This leads

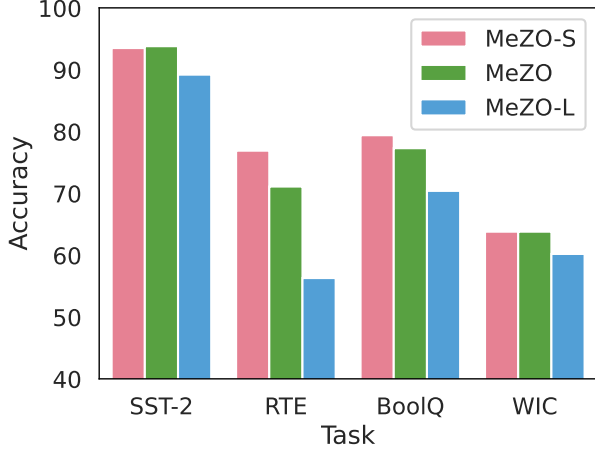


Figure 3. Comparing performance across various parameter adjustments. MeZO: the vanilla MeZO approach, MeZO-S: Fine-Tuning smaller parameters with MeZO, MeZO-L: Fine-Tuning larger parameters with MeZO.

us to examine if perturbations to larger parameters are more critical.

Is the perturbation on larger parameters more important than smaller parameters ?

We conduct experiments to examine how parameter values of varying magnitudes impact performance. Specifically, we set the median value of each layer as a threshold to separate parameters into two groups. Then, we only perturb and update the parameters in one of these groups. For instance, we experiment with updating either just the smaller or larger parameters, using the same settings as the standard MeZO, on SuperGLUE. Then, we compared their performance to that of vanilla MeZO. The results in Figure 3 show that updating only the parameters smaller than the median value leads to better performance on BoolQ, RTE, WIC, and comparable results on SST-2. However, updating only the larger parameters results in significantly worse performance compared to the standard MeZO. This suggests that the key to MeZO’s performance gain lies in the smaller weights.

The reason updating only smaller parameters leads to better performance might be due to the larger weights being well-trained already. Moving them in a random direction is unlikely to enhance performance. On the other hand, since smaller weights are less trained, there’s a higher chance of improvement regardless of the direction of the update.

Based on the observations from Figure 3, we can create a sparse mask, m , determined by parameter magnitudes. Specifically, we employ m to identify and only modify parameters of smaller magnitude. These targeted parameters are defined as $\hat{\theta} = m \odot \theta$. It’s important to note that we still preserve the complete set of parameters, but we apply

Algorithm 1 Sparse-MeZO (S-MeZO)

Require: θ represents pre-trained LLM weight, N is the number of layers in model, learning rate η_t , s represents sparsification interval.
 Initialize random seed s
 Determine threshold $h = h_1, \dots, h_N$, of each layer with the sparsification interval
for $t \leftarrow 1$ **to** T **do**
 Sample Minibatch \mathcal{B} from X and random seed s .
 $m \leftarrow \text{GetMask}(\theta_t, h)$
 $\theta_t \leftarrow \text{PerturbParameters}(\theta_t, \epsilon, s, m)$
 $l^+ = \mathcal{L}(\theta_t; \mathcal{B})$
 $\theta_t \leftarrow \text{PerturbParameters}(\theta_t, -2\epsilon, s, m)$
 $l^- = \mathcal{L}(\theta_t; \mathcal{B})$
 $\theta_t \leftarrow \text{PerturbParameters}(\theta_t, \epsilon, s, m)$
 $\text{proj_grad} \leftarrow (l^+ - l^-)/(2\epsilon)$
 Reset random seed s
 for $\theta_i \in \theta$ **do**
 $z_i \sim \mathcal{N}(0, 1)$
 $\theta_i \leftarrow \theta_i - \eta_t * \text{proj_grad} * m_i * z$
 end for
end for

sparse perturbations and gradient estimations only to the selected ones. This approach allows us to integrate the sparse mask into the standard MeZO method as a straightforward, adaptable tool. Then, we will introduce when and where to calculate the mask.

- **Constant Mask: Setting the Mask Before Training.** We compare the parameter values to a threshold for each layer to set the mask before training begins. However, a significant downside of this approach is the extra memory required to store a sparse mask, which is as large as the pre-trained model itself. Our goal is for our method to enhance performance without using more GPU memory or causing extra overhead.
- **Dynamic Mask: Determining Mask at Each Iteration.** We can establish a threshold for each layer before training and then generate the mask by comparing parameter values to this threshold during each iteration. This method avoids the necessity of storing a large mask, m .

In this paper, we’ll employ a dynamic mask to choose which parameters to perturb and update, addressing the issue of memory constraints.

The pseudo-code is provided in Algorithm 1. This algorithm outlines that we first establish the threshold h_i for each layer before beginning training. We then use GetMask (Algorithm 3) to compare each parameter against its threshold h_i and create the mask m . Following this, we introduce

Algorithm 2 PerturbParameters

Input: θ represents pre-trained LLM weight, perturbation scale ϵ , random seed s , mask m .
 Reset random seed s
for $\theta_i \in \theta$ **do**
 $z_i \sim \mathcal{N}(0, 1)$
 $\theta_i \leftarrow \theta_i + m_i * \epsilon z_i$
end for

Algorithm 3 GetMask

Input: θ represents pre-trained LLM weight, threshold h (h_i represents threshold of each layer).
Output: Mask m
for $i \leftarrow$ Layer 1 **to** Layer N **do**
 for $\theta_{i,j} \in \theta_i$ **do**
 if $\theta_{i,j} \leq h_i$ **then**
 $\theta_{i,j} = 1$
 else
 $\theta_{i,j} = 0$
 end if
 end for
end for

the function PerturbParameters (Algorithm 2) to generate a Gaussian noise sample $z \sim \mathcal{N}(0, I_d)$ and apply the mask m to produce a sparse perturbation $\hat{z} = m \odot z$. With \hat{z} , we perturb the current parameters θ_t to get new parameters $\theta_t + \epsilon \hat{z}$ and $\theta_t - \epsilon \hat{z}$. This allows us to compute two distinct loss values: $l^+ = \mathcal{L}(\theta_t + \epsilon \hat{z})$ and $l^- = \mathcal{L}(\theta_t - \epsilon \hat{z})$. From these losses, we calculate the estimated sparse gradient $g_m(\theta_t) = \text{proj_grad} * \hat{z}$, where $\text{proj_grad} = \frac{l^+ - l^-}{2\epsilon}$. Finally, this gradient can be used with a learning rate η_t to update θ_t .

3.4. Memory-Efficient Implementation of Sparse-MeZO

In this paper, our primary aim is to introduce an efficient method for fine-tuning language models using zeroth-order optimization, enhancing performance on downstream tasks. As outlined in Algorithm 1, our approach involves perturbing the parameters θ_t twice to generate two distinct sets of parameters, $\theta'_t = \theta_t + \epsilon z$ and $\theta''_t = \theta_t - \epsilon z$. We then use the estimated gradient to update the original parameters θ_t . This step typically requires storing two separate sets of parameters, leading to increased memory usage during fine-tuning.

As depicted in Figure 2, recently proposed MeZO, conserves memory by saving random seeds s and using it to resample z for calculating θ'_t , θ''_t , and reconstructing θ_t without needing extra memory. However, applying a sparse mask m for calculating sparse perturbation \hat{z} in MeZO poses a memory issue. We cannot simply reconstruct \hat{z} by saving

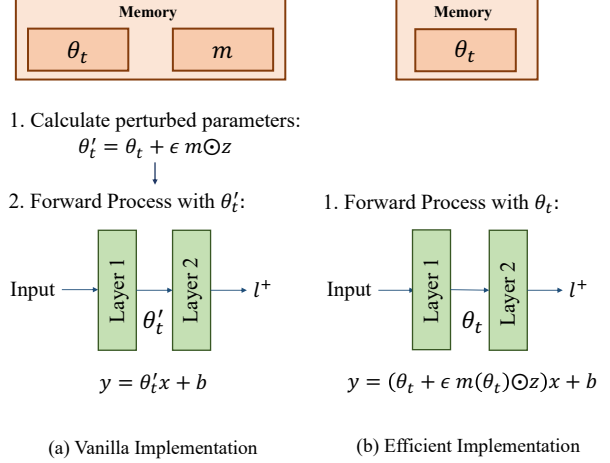


Figure 4. Efficient Implementation of Sparse-MeZO. (a) represents vanilla implementation of S-MeZO, (b) represents our proposed efficient implementation of S-MeZO.

the random seed because the sparse mask, determined by parameter magnitudes, changes when parameters are altered by the perturbation. To address this, we propose potential solutions for the memory issue.

1-bit Quantization: We can apply 1-bit quantization to store the mask m , as it consists solely of 0s and 1s. However, this method still increases memory usage, which isn't our goal. As a solution, we introduce a novel, memory-saving approach for zeroth-order optimization that calculates the mask m on the fly during the forward pass.

Calculating the Mask During the Forward Pass: By computing the mask and perturb parameters in the forward pass, we eliminate the need to store perturbed parameters θ'_t and θ''_t . This means we only have to keep the original parameters θ_t throughout training. We try to compare the difference between vanilla implementation and our proposed efficient implementation in Figure 4. For vanilla implementation, we first need to calculate the perturbed parameters with mask m : $\theta'_t = \theta_t + \epsilon m \odot z$. After that, we can use perturbed parameters θ'_t to calculate the loss value l^+ with the forward process. For example, the output of layer i can be defined as $y^{(i)} = \theta_t^{(i)} x^{(i)} + b^{(i)}$. Noted that we need to save the vanilla parameters θ_t and mask m for vanilla implementation. However, for our proposed efficient implementation, we only need to save vanilla parameters θ_t . More specially, we can calculate the mask $m^{(i)}$ of layer i during the forward process and then obtain the output of this layer: $y^{(i)} = (\theta_t^{(i)} + \epsilon m(\theta_t) z^{(i)}) x^{(i)} + b^{(i)}$, where $m(\cdot)$ represents the function GetMask to calculate mask $m^{(i)}$. Then, we can release the memory about mask $m^{(i)}$ and calculate the output and mask of next layer.

Model	Method	BoolQ	RTE	WIC	MultiRC	SST-2	COPA	Average
LLaMA-7b	Zero-Shot	65.1	49.5	50.6	55.8	79.7	59.7	60.1
LLaMA-7b	ICL	67.4	54.5	52.7	58.7	81.2	84.4	66.5
LLaMA-7b	FT	84.5 ± 0.0	83.6 ± 0.9	68.4 ± 1.3	80.2 ± 1.4	95.7 ± 0.3	85.0 ± 0.8	82.9 ± 0.8
LLaMA-7b	MeZO	75.9 ± 1.1	71.7 ± 1.5	61.4 ± 1.8	69.8 ± 0.7	94.6 ± 0.3	86.3 ± 0.9	76.6 ± 1.1
LLaMA-7b	R-MeZO	76.9 ± 0.7	75.2 ± 1.7	62.1 ± 0.4	68.1 ± 2.0	94.6 ± 0.2	84.3 ± 1.7	76.9 ± 1.1
LLaMA-7b	S-MeZO	80.9 ± 1.6	80.7 ± 1.4	64.9 ± 1.5	73.3 ± 1.2	95.0 ± 0.3	86.7 ± 0.7	80.3 ± 1.2

Table 1. Accuracy of Fine-Tuning LLaMA-7b on SuperGLUE (1,000 examples). ICL: In-Context Learning, FT: full-parameter fine-tuning with Adam, R-MeZO: MeZO with Random Mask.

4. Experiments

Following a similar setting to MeZO, we evaluate the performance of our proposed method on SuperGLUE (Wang et al., 2019). The experimental results show that our proposed method can achieve better performance while also attaining faster convergence.

4.1. Experimental Setting

Datasets. To verify the performance gain of our proposed method, we conduct experiments on various fine-tuning tasks include SST-2 (Socher et al., 2013), RTE (Dagan et al., 2005; Haim et al., 2006; Giampiccolo et al., 2007; Ben-tivogli et al., 2009), BoolQ (Clark et al., 2019), WIC (Pilehvar & Camacho-Collados, 2018), MultiRC (Khashabi et al., 2018)) and multi-class task COPA (Roemmele et al., 2011).

Models. We primarily use pre-trained LLaMA-7b (Touvron et al., 2023) to evaluate the performance of our proposed method on downstream tasks. To further demonstrate our method’s versatility, we also test it with OPT-13b (Zhang et al., 2022). Additionally, to examine our method’s scalability, we evaluate it on larger models, such as LLaMA-30b.

Baselines. First, we compare our method to the vanilla MeZO to demonstrate how sparsification enhances MeZO’s convergence speed and overall performance. Additionally, to show that our proposed S-MeZO effectively identifies and modifies crucial parameters, we contrast it with R-MeZO (a version of MeZO applying a random mask to select parameters for optimization). In addition, we also explore the impact of zero-shot optimization on improving a pre-trained language model’s capabilities through experiments with zeroth-shot learning and in-context learning techniques (Brown et al., 2020). Lastly, to understand the performance gap between zeroth-order and first-order optimization in fine-tuning large language models, we present results from conventional full-parameter fine-tuning (FT) using the Adam optimizer, the most widely used method for such tasks.

Training Procedure. We adopt most of the training hy-

perparameters from the standard MeZO, including dataset configuration, batch size, training epochs, epsilon value, and task prompts, with the key difference being a higher learning rate for S-MeZO due to updating only a subset of the parameters. The primary goal of our training is the next token prediction. For the dataset, we use MeZO’s approach, randomly selecting 1,000 examples for training and testing the model on another set of 1,000 examples (Zhou et al., 2023). We perform the experiments using three different seeds and report the average of the outcomes. In addition, the total training steps for LLaMA and OPT is 20,000 and we evaluate its performance on the test dataset every 100 steps.

4.2. Performance

To evaluate the performance of our proposed method S-MeZO, we initially tested it on the SuperGLUE benchmark using the LLaMA-7b model. The fine-tuning results, presented in Table 1, reveal that our S-MeZO method outperforms other zero-order (ZO) techniques like MeZO and R-MeZO. For instance, S-MeZO boosts MeZO’s accuracy from 71.7% to 80.7% on RTE (↑ 9%) and from 75.9% to 80.9% on BoolQ (↑ 5%). Furthermore, all zeroth-order-based methods surpassed the performance of Zero-shot learning and in-context learning, demonstrating that zeroth-order optimization significantly enhances the pre-trained model’s effectiveness on downstream tasks. Finally, we can find that S-MeZO significantly bridges the performance gap between zero-order and first-order optimization methods.

4.3. Convergence Rate

To verify that S-MeZO converges faster than MeZO, we carried out multiple experiments for comparison. The accuracy over steps is plotted in Figure 5, which shows that S-MeZO can use fewer steps to achieve a better performance than vanilla MeZO. For example, S-MeZO only needs about 5,000 steps to achieve 70% accuracy but vanilla MeZO needs 17,500 steps. Finally, S-MeZO can achieve about 3.5x speedup on RTE and 3x speedup on BoolQ.

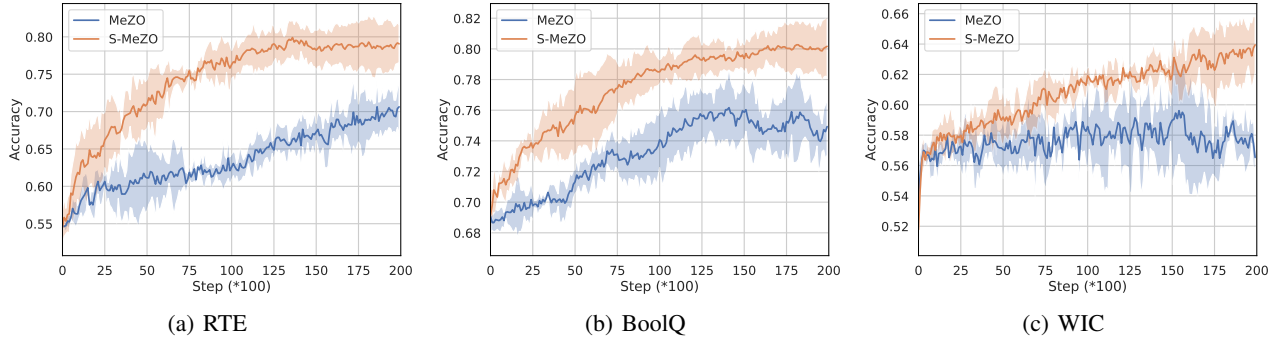


Figure 5. Convergence Curves of Fine-Tuning LLaMA-7b with MeZO and Sparse-MeZO (S-MeZO) on (a) RTE, (b) BoolQ, (c) WIC tasks.

4.4. Memory Usage

Table 2 shows the memory consumption for MeZO, S-MeZO, and traditional full-parameter fine-tuning of LLaMA-7b. The data reveal that S-MeZO does not require more memory than MeZO and offers a substantial saving of roughly 12 times less GPU memory compared to full-parameter fine-tuning. For instance, S-MeZO with Efficient Implementation (S-MeZO-EI) cuts down the memory needed from 158.6 GB for full tuning to just 14.6 GB on MultiRC task. In addition, S-MeZO with efficient implementation can reduce the memory cost from 28.3 GB of vanilla S-MeZO to 14.6 GB across all five tasks, which also illustrates the efficiency of our proposed implementation method: Calculating the Mask During the Forward Pass. Finally, we can only use inference memory cost to fine-tune large language models.

Method	SST-2	RTE	BoolQ	WIC	MultiRC
FT	114.7	123.7	128.7	115.3	158.6
MeZO	14.6	14.6	14.6	14.6	14.6
S-MeZO	28.3	28.3	28.3	28.3	28.3
S-MeZO-EI	14.6	14.6	14.6	14.6	14.6

Table 2. Memory Usage (batch size = 1) of Fine-Tuning LLaMA-7b on SuperGLUE (1,000 examples). EI represents the Efficient Implementation in section 3.4.

4.5. Sparse Rate

For S-MeZO, we need to define the sparsity of the pre-trained model before starting to fine-tune it. To analyze the effects of sparsity value on the performance, we conduct experiments with various sparsity values (from 0.0 to 0.85). Figure 6 summarizes these experimental results with different sparsity values. We can find that a significant performance gain can be obtained when we use the sparsity value from 0.5 to 0.8. In addition, for most tasks, a sparsity

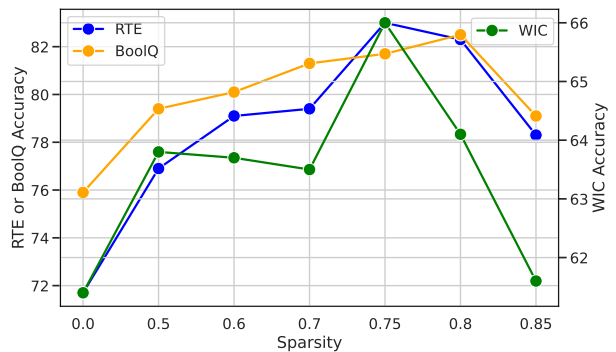


Figure 6. The effects of Sparsity for Fine-tuning LLaMA-7b with S-MeZO.

value of 0.8 or 0.75 usually means a better performance. For example, S-MeZO can improve the accuracy from 71.7% (when $r = 0.0$) to 82.3% (when $r = 0.8$). It can also obtain a performance gain of 6.6% for WIC (from 75.9% to 82.5%).

Model	Method	BoolQ	RTE	WIC
LLaMA-7b	MeZO	75.9	71.7	61.4
LLaMA-7b	S-MeZO	80.9	80.7	64.9
LLaMA-30b	MeZO	83.8	76.9	63.3
LLaMA-30b	S-MeZO	85.7	82.1	67.3

Table 3. Accuracy of Fine-Tuning LLaMA-7b and LLaMA-30b on SuperGLUE (1,000 examples).

4.6. Scalability

In Table 1, we mainly introduce the performance of our methods on LLaMA-7b. A direct question is whether our proposed method can scale to larger language models. Therefore, in this section, we further explore our proposed method S-MeZO on LLaMA-30b. As shown in Table 3, we

can see that the a larger model usually can obtain a better fine-tuned performance. For example, the accuracy on RTE with MeZO can be improved from 71.1% on LLaMA-7b to 76.9% on LLaMA-30b. Our method S-MeZO can further improve the performance on RTE to 82.1% on LLaMA-30b. In addition, S-MeZO can further improve the accuracy on BoolQ to 85.7% on LLaMA-30b.

Model	Method	BoolQ	RTE	WIC
OPT-13b	Zero Shot	59.0	59.6	55.0
OPT-13b	ICL	66.9	62.1	50.5
OPT-13b	MeZO	72.1	75.5	62.2
OPT-13b	R-MeZO	72.3	75.2	61.7
OPT-13b	S-MeZO	73.8	77.6	63.7

Table 4. Accuracy of Fine-Tuning OPT on SuperGLUE (1,000 examples). ICL: In-Context Learning, R-MeZO: MeZO with Random Mask.

4.7. The Analysis about Efficient Implementation

In section 3.4, we present the efficient implementation of S-MeZO, which enables our proposed method to require only the inference memory cost for fine-tuning large language models. To analyze the actual GPU memory usage during the training process, we provide these results in Table 2. We can find that S-MeZO needs the same GPU memory for all five tasks, which can also save about 50% memory compared to sparse-mezo. That also illustrates the efficiency of our proposed efficient implementation.

5. Conclusion

In this paper, we propose a novel memory-efficient zeroth-order fine-tuning method Sparse-MeZO, which can use a similar memory cost to the inference process. We evaluate the performance of fine-tuning LLaMA and OPT with Sparse-MeZO on SuperGULE benchmark and the experimental results illustrate that Sparse-MeZO can achieve a higher accuracy and faster convergence. Finally, we can fine-tune LLaMA-30b in a single A100 GPU. However, there is still a performance gap between our proposed method Sparse-MeZO and first-order fine-tuning methods. We plan to address these limitations and enhance Sparse-MeZO’s capabilities in our future research.

References

Balasubramanian, K. and Ghadimi, S. Zeroth-order (non)-convex stochastic optimization via conditional gradient and gradient updates. *Advances in Neural Information Processing Systems*, 31, 2018.

Bentivogli, L., Clark, P., Dagan, I., and Giampiccolo, D.

The fifth pascal recognizing textual entailment challenge. *TAC*, 7(8):1, 2009.

Brock, A., Lim, T., Ritchie, J. M., and Weston, N. Freeze-out: Accelerate training by progressively freezing layers. *arXiv preprint arXiv:1706.04983*, 2017.

Brown, T., Mann, B., Ryder, N., Subbiah, M., Kaplan, J. D., Dhariwal, P., Neelakantan, A., Shyam, P., Sastry, G., Askell, A., et al. Language models are few-shot learners. *Advances in neural information processing systems*, 33: 1877–1901, 2020.

Cai, H., Gan, C., Zhu, L., and Han, S. Tinytl: Reduce activations, not trainable parameters for efficient on-device learning. *arXiv preprint arXiv:2007.11622*, 2020.

Cai, H., Lou, Y., McKenzie, D., and Yin, W. A zeroth-order block coordinate descent algorithm for huge-scale black-box optimization. In *International Conference on Machine Learning*, pp. 1193–1203. PMLR, 2021.

Cai, H., Mckenzie, D., Yin, W., and Zhang, Z. Zeroth-order regularized optimization (zoro): Approximately sparse gradients and adaptive sampling. *SIAM Journal on Optimization*, 32(2):687–714, 2022.

Chen, A., Zhang, Y., Jia, J., Diffenderfer, J., Liu, J., Parasyris, K., Zhang, Y., Zhang, Z., Kailkhura, B., and Liu, S. Deepzero: Scaling up zeroth-order optimization for deep model training. *arXiv preprint arXiv:2310.02025*, 2023.

Chen, P.-Y., Zhang, H., Sharma, Y., Yi, J., and Hsieh, C.-J. Zoo: Zeroth order optimization based black-box attacks to deep neural networks without training substitute models. In *Proceedings of the 10th ACM workshop on artificial intelligence and security*, pp. 15–26, 2017.

Clark, C., Lee, K., Chang, M.-W., Kwiatkowski, T., Collins, M., and Toutanova, K. Boolq: Exploring the surprising difficulty of natural yes/no questions. *arXiv preprint arXiv:1905.10044*, 2019.

Dagan, I., Glickman, O., and Magnini, B. The pascal recognizing textual entailment challenge. In *Machine learning challenges workshop*, pp. 177–190. Springer, 2005.

Duchi, J. C., Jordan, M. I., Wainwright, M. J., and Wibisono, A. Optimal rates for zero-order convex optimization: The power of two function evaluations. *IEEE Transactions on Information Theory*, 61(5):2788–2806, 2015.

Frankle, J. and Carbin, M. The lottery ticket hypothesis: Finding sparse, trainable neural networks. *arXiv preprint arXiv:1803.03635*, 2018.

- Giampiccolo, D., Magnini, B., Dagan, I., and Dolan, W. B. The third pascal recognizing textual entailment challenge. In *Proceedings of the ACL-PASCAL workshop on textual entailment and paraphrasing*, pp. 1–9, 2007.
- Gu, J., Feng, C., Zhao, Z., Ying, Z., Chen, R. T., and Pan, D. Z. Efficient on-chip learning for optical neural networks through power-aware sparse zeroth-order optimization. In *Proceedings of the AAAI conference on artificial intelligence*, volume 35, pp. 7583–7591, 2021.
- Haim, R. B., Dagan, I., Dolan, B., Ferro, L., Giampiccolo, D., Magnini, B., and Szpektor, I. The second pascal recognising textual entailment challenge. In *Proceedings of the Second PASCAL Challenges Workshop on Recognising Textual Entailment*, volume 7, pp. 785–794, 2006.
- Han, S., Mao, H., and Dally, W. J. Deep compression: Compressing deep neural networks with pruning, trained quantization and huffman coding. *arXiv preprint arXiv:1510.00149*, 2015a.
- Han, S., Pool, J., Tran, J., and Dally, W. Learning both weights and connections for efficient neural network. *Advances in neural information processing systems*, 28, 2015b.
- Hanson, S. and Pratt, L. Comparing biases for minimal network construction with back-propagation. *Advances in neural information processing systems*, 1, 1988.
- Hassibi, B. and Stork, D. Second order derivatives for network pruning: Optimal brain surgeon. *Advances in neural information processing systems*, 5, 1992.
- Houlsby, N., Giurgiu, A., Jastrzebski, S., Morrone, B., De Laroussilhe, Q., Gesmundo, A., Attariyan, M., and Gelly, S. Parameter-efficient transfer learning for nlp. In *International Conference on Machine Learning*, pp. 2790–2799. PMLR, 2019.
- Hu, E. J., Shen, Y., Wallis, P., Allen-Zhu, Z., Li, Y., Wang, S., Wang, L., and Chen, W. Lora: Low-rank adaptation of large language models. *arXiv preprint arXiv:2106.09685*, 2021.
- Ilyas, A., Engstrom, L., Athalye, A., and Lin, J. Black-box adversarial attacks with limited queries and information. In *International conference on machine learning*, pp. 2137–2146. PMLR, 2018.
- Khashabi, D., Chaturvedi, S., Roth, M., Upadhyay, S., and Roth, D. Looking beyond the surface: A challenge set for reading comprehension over multiple sentences. In *Proceedings of the 2018 Conference of the North American Chapter of the Association for Computational Linguistics: Human Language Technologies, Volume 1 (Long Papers)*, pp. 252–262, 2018.
- LeCun, Y., Denker, J., and Solla, S. Optimal brain damage. *Advances in neural information processing systems*, 2, 1989.
- Lester, B., Al-Rfou, R., and Constant, N. The power of scale for parameter-efficient prompt tuning. *arXiv preprint arXiv:2104.08691*, 2021.
- Li, X. L. and Liang, P. Prefix-tuning: Optimizing continuous prompts for generation. *arXiv preprint arXiv:2101.00190*, 2021.
- Lin, Z., Madotto, A., and Fung, P. Exploring versatile generative language model via parameter-efficient transfer learning. *arXiv preprint arXiv:2004.03829*, 2020.
- Liu, H., Tam, D., Muqeeth, M., Mohta, J., Huang, T., Bansal, M., and Raffel, C. A. Few-shot parameter-efficient fine-tuning is better and cheaper than in-context learning. *Advances in Neural Information Processing Systems*, 35: 1950–1965, 2022.
- Liu, S., Kailkhura, B., Chen, P.-Y., Ting, P., Chang, S., and Amini, L. Zeroth-order stochastic variance reduction for nonconvex optimization. *Advances in Neural Information Processing Systems*, 31, 2018.
- Liu, S., Chen, P.-Y., Chen, X., and Hong, M. signsgd via zeroth-order oracle. In *International conference on learning representations*. International Conference on Learning Representations, ICLR, 2019.
- Liu, S., Chen, P.-Y., Kailkhura, B., Zhang, G., Hero III, A. O., and Varshney, P. K. A primer on zeroth-order optimization in signal processing and machine learning: Principals, recent advances, and applications. *IEEE Signal Processing Magazine*, 37(5):43–54, 2020.
- Liu, Y., Agarwal, S., and Venkataraman, S. Autofreeze: Automatically freezing model blocks to accelerate fine-tuning. *arXiv preprint arXiv:2102.01386*, 2021.
- Malladi, S., Gao, T., Nichani, E., Damian, A., Lee, J. D., Chen, D., and Arora, S. Fine-tuning language models with just forward passes. *arXiv preprint arXiv:2305.17333*, 2023.
- Ohta, M., Berger, N., Sokolov, A., and Riezler, S. Sparse perturbations for improved convergence in stochastic zeroth-order optimization. In *Machine Learning, Optimization, and Data Science: 6th International Conference, LOD 2020, Siena, Italy, July 19–23, 2020, Revised Selected Papers, Part II 6*, pp. 39–64. Springer, 2020.
- Pilehvar, M. T. and Camacho-Collados, J. Wic: the word-in-context dataset for evaluating context-sensitive meaning representations. *arXiv preprint arXiv:1808.09121*, 2018.

- Rebuffi, S.-A., Bilen, H., and Vedaldi, A. Learning multiple visual domains with residual adapters. *Advances in neural information processing systems*, 30, 2017.
- Roemmele, M., Bejan, C. A., and Gordon, A. S. Choice of plausible alternatives: An evaluation of commonsense causal reasoning. In *2011 AAAI Spring Symposium Series*, 2011.
- Ruan, Y., Xiong, Y., Reddi, S., Kumar, S., and Hsieh, C.-J. Learning to learn by zeroth-order oracle. *arXiv preprint arXiv:1910.09464*, 2019.
- Socher, R., Perelygin, A., Wu, J., Chuang, J., Manning, C. D., Ng, A. Y., and Potts, C. Recursive deep models for semantic compositionality over a sentiment treebank. In *Proceedings of the 2013 conference on empirical methods in natural language processing*, pp. 1631–1642, 2013.
- Spall, J. C. Multivariate stochastic approximation using a simultaneous perturbation gradient approximation. *IEEE transactions on automatic control*, 37(3):332–341, 1992.
- Ström, N. Phoneme probability estimation with dynamic sparsely connected artificial neural networks. *The Free Speech Journal*, 5(1-41):2, 1997.
- Sun, T., He, Z., Qian, H., Zhou, Y., Huang, X.-J., and Qiu, X. Bbtv2: towards a gradient-free future with large language models. In *Proceedings of the 2022 Conference on Empirical Methods in Natural Language Processing*, pp. 3916–3930, 2022a.
- Sun, T., Shao, Y., Qian, H., Huang, X., and Qiu, X. Black-box tuning for language-model-as-a-service. In *International Conference on Machine Learning*, pp. 20841–20855. PMLR, 2022b.
- Sung, Y.-L., Cho, J., and Bansal, M. Lst: Ladder side-tuning for parameter and memory efficient transfer learning. *Advances in Neural Information Processing Systems*, 35: 12991–13005, 2022.
- Touvron, H., Lavril, T., Izacard, G., Martinet, X., Lachaux, M.-A., Lacroix, T., Rozière, B., Goyal, N., Hambro, E., Azhar, F., et al. Llama: Open and efficient foundation language models. *arXiv preprint arXiv:2302.13971*, 2023.
- Tu, C.-C., Ting, P., Chen, P.-Y., Liu, S., Zhang, H., Yi, J., Hsieh, C.-J., and Cheng, S.-M. Autozoom: Autoencoder-based zeroth order optimization method for attacking black-box neural networks. In *Proceedings of the AAAI Conference on Artificial Intelligence*, volume 33, pp. 742–749, 2019.
- Vemula, A., Sun, W., and Bagnell, J. Contrasting exploration in parameter and action space: A zeroth-order optimization perspective. In *The 22nd International Conference on Artificial Intelligence and Statistics*, pp. 2926–2935. PMLR, 2019.
- Wang, A., Pruksachatkun, Y., Nangia, N., Singh, A., Michael, J., Hill, F., Levy, O., and Bowman, S. Super-glue: A stickier benchmark for general-purpose language understanding systems. *Advances in neural information processing systems*, 32, 2019.
- Wang, X., Guo, W., Su, J., Yang, X., and Yan, J. Zarts: On zero-order optimization for neural architecture search. *Advances in Neural Information Processing Systems*, 35: 12868–12880, 2022.
- Wang, Y., Du, S., Balakrishnan, S., and Singh, A. Stochastic zeroth-order optimization in high dimensions. In *International conference on artificial intelligence and statistics*, pp. 1356–1365. PMLR, 2018.
- Ye, H., Huang, Z., Fang, C., Li, C. J., and Zhang, T. Hessian-aware zeroth-order optimization for black-box adversarial attack. *arXiv preprint arXiv:1812.11377*, 2018.
- Zaken, E. B., Ravfogel, S., and Goldberg, Y. Bitfit: Simple parameter-efficient fine-tuning for transformer-based masked language-models. *arXiv preprint arXiv:2106.10199*, 2021.
- Zhang, Q., Chen, M., Bukharin, A., He, P., Cheng, Y., Chen, W., and Zhao, T. Adaptive budget allocation for parameter-efficient fine-tuning. *arXiv preprint arXiv:2303.10512*, 2023.
- Zhang, S., Roller, S., Goyal, N., Artetxe, M., Chen, M., Chen, S., Dewan, C., Diab, M., Li, X., Lin, X. V., et al. Opt: Open pre-trained transformer language models. *arXiv preprint arXiv:2205.01068*, 2022.
- Zhou, C., Liu, P., Xu, P., Iyer, S., Sun, J., Mao, Y., Ma, X., Efrat, A., Yu, P., Yu, L., et al. Lima: Less is more for alignment. *arXiv preprint arXiv:2305.11206*, 2023.

A. The Prompts in LLaMA and OPT

Dataset	Type	Prompt
SST-2	cls.	{premise} Does this mean that “{hypothesis}” is true? Yes or No? Yes/No
RTE	cls.	Suppose “{premise}” Can we infer that “{hypothesis}”? Yes, No, or Maybe? Yes/No/Maybe
BoolQ	cls.	{passage} {question} ? Yes/No
WIC	cls.	Does the word “{word}” have the same meaning in these two sentences? Yes, No? {sent1} {sent2} Yes/No
MultiRC	cls.	{paragraph} Question: {question} I found this answer “{answer}”. Is that correct? Yes or No? Yes/No
COPA	mch.	{premise} so/because {candidate}

Table 5. The prompts of the datasets we used in our LLaMA experiments.

B. Hyperparameters

We will introduce the hyperparameters searching grids in Table 6, which can help people to reproduce our results.

Experiment	Hyperparameters	Values
MeZO	Batch size	16
	Learning rate	{5e-7, 1e-6, 2e-6}
	ϵ	1e-3
MeZO-Random	Batch size	16
	Learning rate	{1e-6, 2e-6, 3e-6, 4e-6, 5e-6}
	ϵ	1e-3
S-MeZO	Batch size	16
	Learning rate	{1e-6, 2e-6, 3e-6, 4e-6, 5e-6}
	ϵ	1e-3
FT with Adam	Batch size	8
	Learning Rates	{1e-5, 5e-5, 8e-5}

Table 6. The hyperparameter searching grids for LLaMA-7b experiments.

We then introduce the sparsity of each task in SuperGULU when we fine-tune LLaMA-7b.

Method	SST-2	RTE	BoolQ	WIC	MultiRC
Sparse MeZO	0.70	0.75	0.80	0.80	0.80

Table 7. Sparsity in SuperGULU when we fine-tune LLaMA-7b.

C. The Proof of Lemma 3.2

Let $\mathcal{L}_z(\theta)$ be the expectation of $\mathcal{L}(\theta + \epsilon m \odot z)$:

$$\begin{aligned}\mathcal{L}_{\hat{z}}(\theta) &:= \mathbb{E}_z[\mathcal{L}(\theta + \epsilon m \odot z)] \\ &= \mathbb{E}_{\hat{z}}[\mathcal{L}(\theta + \epsilon \hat{z})]\end{aligned}\tag{8}$$

We can obtain the Lemma:

$$\begin{aligned}\widehat{\nabla}_\theta \mathcal{L}_{\hat{z}}(\theta) &= m \odot \nabla_\theta \mathcal{L}_{\hat{z}}(\theta) \\ &= m \odot \mathbb{E}_z[\nabla_\theta \mathcal{L}(\theta + \epsilon m \odot z)] \\ &= \mathbb{E}_z\left[\frac{\mathcal{L}(\theta + \epsilon m \odot z) - \mathcal{L}(\theta - \epsilon m \odot z)}{2\epsilon} m \odot z\right] \\ &= \mathbb{E}_{\hat{z}}\left[\frac{\mathcal{L}(\theta + \epsilon \hat{z}) - \mathcal{L}(\theta - \epsilon \hat{z})}{2\epsilon} \hat{z}\right]\end{aligned}\tag{9}$$

Proof:

$$\begin{aligned}\widehat{\nabla}_\theta \mathcal{L}_{\hat{z}}(\theta) &= \widehat{\nabla}_\theta \mathbb{E}_{\hat{z}}[\mathcal{L}(\theta + \epsilon \hat{z})] \\ &= \widehat{\nabla}_\theta \int_{\hat{z}} \text{pdf}_{\hat{z}}(z) \mathcal{L}(\theta + \epsilon z) dz \\ &= m \odot \nabla_\theta \int_{\hat{z}} \text{pdf}_{\hat{z}}(z) \mathcal{L}(\theta + \epsilon z) dz \\ &= m \odot \int_{\hat{z}} \nabla_\theta \text{pdf}_{\hat{z}}(z) \mathcal{L}(\theta + \epsilon z) dz \\ &= \frac{1}{k} m \odot \int_{\hat{z}} \nabla_\theta e^{-\frac{1}{2}\|z\|^2} \mathcal{L}(\theta + \epsilon z) dz \\ &= \frac{1}{k} m \odot \int_{\hat{y}} \nabla_\theta e^{-\frac{1}{2}\|\frac{y-\theta}{\epsilon}\|^2} \mathcal{L}(y) \frac{1}{\epsilon^n} dy \\ &= \frac{1}{k} m \odot \int_{\hat{y}} \frac{y-\theta}{\epsilon^2} e^{-\frac{1}{2\epsilon^2}\|y-\theta\|^2} \mathcal{L}(y) \frac{1}{\epsilon^n} dy \\ &= \frac{1}{k} m \odot \int_{\hat{z}} \frac{\hat{z}}{\epsilon} e^{-\frac{1}{2}\|z\|^2} \mathcal{L}(\theta + \epsilon z) dz \\ &= m \odot \int_{\hat{z}} \text{pdf}_{\hat{z}}(z) \mathcal{L}(\theta + \epsilon z) \frac{\hat{z}}{\epsilon} dz \\ &= \mathbb{E}_{\hat{z}}\left[m \odot \frac{\mathcal{L}(\theta + \epsilon \hat{z})}{\epsilon} \hat{z}\right] \\ &= \mathbb{E}_{\hat{z}}\left[\frac{\mathcal{L}(\theta + \epsilon \hat{z})}{\epsilon} \hat{z}\right]\end{aligned}\tag{10}$$

where we can define $y = \theta + \epsilon z$, $\hat{y} = \theta + \epsilon m \odot z$, $k = \sqrt{(2\pi)^{\hat{d}}}$ and \hat{d} is the number of 1 in m .

Therefore, we can obtain the gradient $\nabla_\theta \mathcal{L}_m(\theta)$ is equal to $\mathbb{E}_{\hat{z}}\left[\frac{\mathcal{L}(\theta + \epsilon \hat{z})}{\epsilon} \hat{z}\right]$.

In addition, we will prove $\mathbb{E}_{\hat{z}}\left[\frac{\mathcal{L}(\theta + \epsilon \hat{z})}{\epsilon} \hat{z}\right]$ is also equal to $\mathbb{E}_{\hat{z}}\left[\frac{\mathcal{L}(\theta + \epsilon \hat{z}) - \mathcal{L}(\theta)}{\epsilon} \hat{z}\right]$:

$$\begin{aligned}
 & \mathbb{E}_{\hat{z}} \left[\frac{\mathcal{L}(\theta + \epsilon \hat{z}) - \mathcal{L}(\theta)}{\epsilon} \hat{z} \right] \\
 &= \frac{1}{k} \int_{\hat{z}} \frac{\mathcal{L}(\theta + \epsilon z) - \mathcal{L}(\theta)}{\epsilon} z e^{-\frac{1}{2} \|z\|^2} dz \\
 &= \frac{1}{k} \int_{\hat{z}} \frac{\mathcal{L}(\theta + \epsilon z)}{\epsilon} z e^{-\frac{1}{2} \|z\|^2} dz - \frac{\mathcal{L}(\theta)}{\epsilon k} \int_{\hat{z}} z e^{-\frac{1}{2} \|z\|^2} dz \\
 &= \mathbb{E}_{\hat{z}} \left[\frac{\mathcal{L}(\theta + \epsilon \hat{z})}{\epsilon} \hat{z} \right]
 \end{aligned} \tag{11}$$

After that, we can get the relationship between $\mathbb{E}_{\hat{z}} \left[\frac{\mathcal{L}(\theta) - \mathcal{L}(\theta - \epsilon \hat{z})}{\epsilon} \hat{z} \right]$ and $\mathbb{E}_{\hat{z}} \left[\frac{\mathcal{L}(\theta + \epsilon \hat{z})}{\epsilon} \hat{z} \right]$:

$$\begin{aligned}
 \mathbb{E}_{\hat{z}} \left[\frac{\mathcal{L}(\theta) - \mathcal{L}(\theta - \epsilon \hat{z})}{\epsilon} \hat{z} \right] &= \mathbb{E}_{\hat{z}} \left[\frac{\mathcal{L}(\theta + \epsilon(-\hat{z})) - \mathcal{L}(\theta)}{\epsilon} (-\hat{z}) \right] \\
 &= \mathbb{E}_{\hat{z}} \left[\frac{\mathcal{L}(\theta + \epsilon \hat{z} - \mathcal{L}(\theta))}{\epsilon} \hat{z} \right] \\
 &= \mathbb{E}_{\hat{z}} \left[\frac{\mathcal{L}(\theta + \epsilon \hat{z})}{\epsilon} \hat{z} \right].
 \end{aligned} \tag{12}$$

Based on the Equation 11 and Equation 12, we can obtain:

$$\begin{aligned}
 & \mathbb{E}_{\hat{z}} \left[\frac{\mathcal{L}(\theta + \epsilon \hat{z}) - \mathcal{L}(\theta - \epsilon \hat{z})}{2\epsilon} \hat{z} \right] \\
 &= \frac{1}{2} \left(\mathbb{E}_{\hat{z}} \left[\frac{\mathcal{L}(\theta + \epsilon \hat{z})}{\epsilon} \hat{z} - \frac{\mathcal{L}(\theta)}{\epsilon} \hat{z} + \frac{\mathcal{L}(\theta)}{\epsilon} \hat{z} - \frac{\mathcal{L}(\theta - \epsilon \hat{z})}{\epsilon} \hat{z} \right] \right) \\
 &= \frac{1}{2} \left(\mathbb{E}_{\hat{z}} \left[\frac{\mathcal{L}(\theta + \epsilon \hat{z}) - \mathcal{L}(\theta)}{\epsilon} \hat{z} \right] + \mathbb{E}_{\hat{z}} \left[\frac{\mathcal{L}(\theta) - \mathcal{L}(\theta - \epsilon \hat{z})}{\epsilon} \hat{z} \right] \right) \\
 &= \frac{1}{2} \left(\mathbb{E}_{\hat{z}} \left[\frac{\mathcal{L}(\theta + \epsilon \hat{z})}{\epsilon} \hat{z} \right] + \mathbb{E}_{\hat{z}} \left[\frac{\mathcal{L}(\theta + \epsilon \hat{z})}{\epsilon} \hat{z} \right] \right) \\
 &= \mathbb{E}_{\hat{z}} \left[\frac{\mathcal{L}(\theta + \epsilon \hat{z})}{\epsilon} \hat{z} \right] \\
 &= \widehat{\nabla}_{\theta} \mathcal{L}_{\hat{z}}(\theta)
 \end{aligned} \tag{13}$$

Finally, we can obtain the relationship between $\mathbb{E}_{\hat{z}} \left[\frac{\mathcal{L}(\theta + \epsilon \hat{z}) - \mathcal{L}(\theta - \epsilon \hat{z})}{2\epsilon} \hat{z} \right]$ and $\widehat{\nabla}_{\theta} \mathcal{L}_{\hat{z}}(\theta)$ and finish the proof.

D. The Proof of Lemma 3.3

$$\|\nabla_{\theta} \mathcal{L}_m(\theta)\|^2 \leq 2\|\widehat{\nabla}_{\theta} \mathcal{L}_{\hat{z}}(\theta)\|^2 + \frac{\epsilon^2 L^2(l)}{2} (\hat{d} + 4)^3. \tag{14}$$

Proof:

We can first define the distance between $\widehat{\nabla}_{\theta} \mathcal{L}_{\hat{z}}(\theta) = \mathbb{E}_{\hat{z}} [\mathbf{g}_{\hat{z}}(\theta)]$ and sparse FO gradient $\nabla \mathcal{L}_m(\theta)$ as:

$$\begin{aligned}
 & \|\widehat{\nabla}_\theta \mathcal{L}_{\hat{z}}(\theta) - \nabla_\theta \mathcal{L}_m(\theta)\| \\
 &= \left\| \frac{1}{k} \int_z \left(\frac{\mathcal{L}(\theta + \epsilon z) - \mathcal{L}(\theta - \epsilon z)}{2\epsilon} - \langle \nabla_\theta \mathcal{L}_m(\theta), z \rangle \right) z e^{-\frac{1}{2}\|z\|^2} dz \right\| \\
 &= \left\| \frac{1}{k} \int_z \left(\frac{\mathcal{L}(\theta + \epsilon z) - \mathcal{L}(\theta)}{\epsilon} - \langle m \odot \nabla_\theta \mathcal{L}(\theta), z \rangle \right) z e^{-\frac{1}{2}\|z\|^2} dz \right\| \\
 &\leq \frac{1}{k\epsilon} \int_z \|\mathcal{L}(\theta + \epsilon z) - \mathcal{L}(\theta) - \epsilon \langle \nabla_\theta \mathcal{L}(\theta), \epsilon \rangle\| \|m \odot z\| e^{-\frac{1}{2}\|z\|^2} dz \\
 &\leq \frac{\epsilon L(l)}{2k} \int_\epsilon \|z\|^2 \|m \odot z\| e^{-\frac{1}{2}\|z\|^2} dz \\
 &= \frac{\epsilon L(l)}{2} \mathbb{E}_{\hat{z}}[\|\hat{z}\|^3] \\
 &\leq \frac{\epsilon L(l)}{2} (\hat{d} + 3)^{\frac{3}{2}}
 \end{aligned} \tag{15}$$

where \hat{d} is the number of selected parameters with mask \mathbf{m} . In addition, $\|\mathbf{a} + \mathbf{b}\|^2 \leq 2\|\mathbf{a}\|^2 + 2\|\mathbf{b}\|^2$, we can define $\mathbf{a} = \mathbf{a} - \mathbf{b}$ and obtain that $\|\mathbf{a}\|^2 \leq 2\|\mathbf{a} - \mathbf{b}\|^2 + 2\|\mathbf{b}\|^2$. Let $\mathbf{a} = \nabla_\theta \mathcal{L}_m(\theta)$ and $\mathbf{b} = \widehat{\nabla}_\theta \mathcal{L}_{\hat{z}}(\theta)$, we can obtain:

$$\begin{aligned}
 \|\nabla_\theta \mathcal{L}_m(\theta)\|^2 &\leq 2\|\widehat{\nabla}_\theta \mathcal{L}_{\hat{z}}(\theta) - \nabla_\theta \mathcal{L}_m(\theta)\|^2 + 2\|\widehat{\nabla}_\theta \mathcal{L}_{\hat{z}}(\theta)\|^2 \\
 &\leq \frac{\epsilon^2 L^2(l)}{2} (\hat{d} + 3)^3 + 2\|\widehat{\nabla}_\theta \mathcal{L}_{\hat{z}}(\theta)\|^2 \\
 &\leq \frac{\epsilon^2 L^2(l)}{2} (\hat{d} + 4)^3 + 2\|\widehat{\nabla}_\theta \mathcal{L}_{\hat{z}}(\theta)\|^2
 \end{aligned} \tag{16}$$

E. The Proof of Theorem 3.4

Proof:

$$\begin{aligned}
 \mathcal{L}_{\hat{z}}(\theta) - \mathcal{L}(\theta) &= \mathbb{E}_{\hat{z}}[\mathcal{L}(\theta + \epsilon \hat{z}) - \mathcal{L}(\theta)] \\
 &= \mathbb{E}_{\hat{z}}[\mathcal{L}(\theta + \epsilon \hat{z}) - \mathcal{L}(\theta) - \epsilon \langle \nabla \mathcal{L}(\theta), \hat{z} \rangle] \\
 &= \frac{1}{k} \int_{\hat{z}} [\mathcal{L}(\theta + \epsilon z) - \mathcal{L}(\theta) - \epsilon \langle \nabla \mathcal{L}(\theta), z \rangle] e^{-\frac{1}{2}\|z\|^2} dz \\
 &\leq \frac{1}{k} \int_{\hat{z}} \frac{\epsilon^2 L(l)}{2} \|z\|^2 e^{-\frac{1}{2}\|z\|^2} dz \\
 &= \frac{\epsilon^2 L(l)}{2} \mathbb{E}_{\hat{z}}[\|\hat{z}\|^2] \\
 &\leq \frac{\epsilon^2 L(l)}{2} \hat{d}
 \end{aligned} \tag{17}$$

The first inequality holds because Lipschitz Continuous: $|\mathcal{L}(\theta') - \mathcal{L}(\theta) - \langle \nabla \mathcal{L}(\theta), \theta' - \theta \rangle| \leq \frac{L(l)}{2} \|\theta' - \theta\|^2$, where $\theta' = \theta + \epsilon z$. The second inequality holds because $\mathbb{E}_{\hat{z}}[\|\hat{z}\|^2] = \hat{d}$, where \hat{d} is the number of 1 in mask \mathbf{m} .

$$\begin{aligned}
 & [(\mathcal{L}_{\hat{z}}(\theta) - \mathcal{L}(\theta)) - (\mathcal{L}_{\hat{z}}(\theta + \epsilon \hat{z}) - \mathcal{L}(\theta + \epsilon \hat{z}))]^2 \\
 &\leq 2[\mathcal{L}_{\hat{z}}(\theta) - \mathcal{L}(\theta)]^2 + 2[\mathcal{L}_{\hat{z}}(\theta + \epsilon \hat{z}) - \mathcal{L}(\theta + \epsilon \hat{z})]^2 \\
 &\leq \frac{\epsilon^4 L^2(l)}{2} \hat{d}^2 + \frac{\epsilon^4 L^2(l)}{2} \hat{d}^2 \\
 &= \epsilon^4 L^2(l) \hat{d}^2
 \end{aligned} \tag{18}$$

The first inequality is due to $\|\mathbf{a} + \mathbf{b}\|^2 \leq 2\|\mathbf{a}\|^2 + 2\|\mathbf{b}\|^2$, where $\mathbf{a} = \mathcal{L}_{\hat{z}}(\theta) - \mathcal{L}(\theta)$, $\mathbf{b} = \mathcal{L}_{\hat{z}}(\theta + \epsilon \hat{z}) - \mathcal{L}(\theta + \epsilon \hat{z})$. The

second inequality is due to the Equation 17.

$$\begin{aligned}
 [\mathcal{L}_{\hat{z}}(\theta + \epsilon\hat{z}) - \mathcal{L}_{\hat{z}}(\theta)]^2 &\leq 2[\mathcal{L}_{\hat{z}}(\theta + \epsilon\hat{z}) - \mathcal{L}_{\hat{z}}(\theta) - \epsilon\langle \widehat{\nabla}_{\theta} \mathcal{L}_{\hat{z}}(\theta), \hat{z} \rangle]^2 + 2[\epsilon\langle \widehat{\nabla}_{\theta} \mathcal{L}_{\hat{z}}(\theta), \hat{z} \rangle]^2 \\
 &\leq \frac{\epsilon^4 L^2(l)}{2} \|\hat{z}\|^4 + 2\epsilon^2 \langle \widehat{\nabla}_{\theta} \mathcal{L}_{\hat{z}}(\theta), \hat{z} \rangle^2 \\
 &\leq \frac{\epsilon^4 L^2(l)}{2} \|\hat{z}\|^4 + 2\epsilon^2 \|\widehat{\nabla}_{\theta} \mathcal{L}_{\hat{z}}(\theta)\|^2 \|\hat{z}\|^2
 \end{aligned} \tag{19}$$

The first inequality is due to $\|\mathbf{a} + \mathbf{b}\|^2 \leq 2\|\mathbf{a}\|^2 + 2\|\mathbf{b}\|^2$. The second inequality holds because Lipschitz Continuous: $|\mathcal{L}(\theta') - \mathcal{L}(\theta) - \langle \nabla \mathcal{L}(\theta), \theta' - \theta \rangle| \leq \frac{L(l)}{2} \|\theta' - \theta\|^2$, where $\theta' = \theta + \epsilon\hat{z}$.

$$\begin{aligned}
 &[\mathcal{L}(\theta + \epsilon\hat{z}) - \mathcal{L}(\theta)]^2 \\
 &\leq 2[(\mathcal{L}_{\hat{z}}(\theta) - \mathcal{L}(\theta)) - (\mathcal{L}_{\hat{z}}(\theta + \epsilon\hat{z}) - \mathcal{L}(\theta + \epsilon\hat{z}))]^2 + 2[\mathcal{L}_{\hat{z}}(\theta + \epsilon\hat{z}) - \mathcal{L}_{\hat{z}}(\theta)]^2 \\
 &\leq 2\epsilon^4 L^2(l) \hat{d}^2 + \epsilon^4 L^2(l) \|\hat{z}\|^4 + 4\epsilon^2 \|\widehat{\nabla}_{\theta} \mathcal{L}_{\hat{z}}(\theta)\|^2 \|\hat{z}\|^2
 \end{aligned} \tag{20}$$

The first inequality is due to $\|\mathbf{a} + \mathbf{b}\|^2 \leq 2\|\mathbf{a}\|^2 + 2\|\mathbf{b}\|^2$. The last inequality holds because Equation 18 and Equation 19.

$$\begin{aligned}
 \mathbb{E}_{z,x}[\|g_{\hat{z}}(\theta)\|^2] &= \mathbb{E}_{\hat{z}}\left[\left\|\frac{\mathcal{L}(\theta + \epsilon\hat{z}) - \mathcal{L}(\theta - \epsilon\hat{z})}{2\epsilon} \hat{z}\right\|^2\right] \\
 &= \mathbb{E}_{\hat{z}}\left[\left\|\frac{\mathcal{L}(\theta + \epsilon\hat{z}) - \mathcal{L}(\theta)}{2\epsilon} \hat{z} + \frac{\mathcal{L}(\theta) - \mathcal{L}(\theta - \epsilon\hat{z})}{2\epsilon} \hat{z}\right\|^2\right] \\
 &\leq \mathbb{E}_{\hat{z}}\left[2\left\|\frac{\mathcal{L}(\theta + \epsilon\hat{z}) - \mathcal{L}(\theta)}{2\epsilon} \hat{z}\right\|^2 + 2\left\|\frac{\mathcal{L}(\theta) - \mathcal{L}(\theta - \epsilon\hat{z})}{2\epsilon} \hat{z}\right\|^2\right] \\
 &= \mathbb{E}_{\hat{z}}\left[\frac{1}{2\epsilon^2} [\mathcal{L}(\theta + \epsilon\hat{z}) - \mathcal{L}(\theta)]^2 \cdot \|\hat{z}\|^2 + \frac{1}{2\epsilon^2} [\mathcal{L}(\theta) - \mathcal{L}(\theta - \epsilon\hat{z})]^2 \cdot \|\hat{z}\|^2\right] \\
 &\leq \mathbb{E}_{\hat{z}}[2\epsilon^2 L^2(l) \hat{d}^2 \|\hat{z}\|^2 + \epsilon^2 L^2(l) \|\hat{z}\|^6 + 4\|\widehat{\nabla} \mathcal{L}_{\hat{z}}(\theta)\|^2 \|\hat{z}\|^4] \\
 &\leq 2\epsilon^2 L^2(l) \hat{d}^3 + \epsilon^2 L^2(l) (\hat{d} + 6)^3 + 4(\hat{d} + 4)^2 \|\widehat{\nabla} \mathcal{L}_{\hat{z}}(\theta)\|^2 \\
 &\leq 3\epsilon^2 L^2(l) (\hat{d} + 4)^3 + 4(\hat{d} + 4)^2 \|\widehat{\nabla} \mathcal{L}_{\hat{z}}(\theta)\|^2
 \end{aligned} \tag{21}$$

The first inequality holds because $\|\mathbf{a} + \mathbf{b}\|^2 \leq 2\|\mathbf{a}\|^2 + 2\|\mathbf{b}\|^2$, where $\mathbf{a} = \frac{\mathcal{L}(\theta + \epsilon\hat{z}) - \mathcal{L}(\theta)}{2\epsilon} \hat{z}$, $\mathbf{b} = \frac{\mathcal{L}(\theta) - \mathcal{L}(\theta - \epsilon\hat{z})}{2\epsilon} \hat{z}$. The second inequality is due to the Equation 20. The third inequality holds because $\mathbb{E}_{\hat{z}}[\|\hat{z}\|^2] = \hat{d}$, $\mathbb{E}_{\hat{z}}[\|\hat{z}\|^p] \leq (\hat{d} + p)^{\frac{p}{2}}$ for $p \geq 2$. The last inequality holds because $2\hat{d}^3 + (\hat{d} + 6)^3 \leq 3(\hat{d} + 4)^3$.

Based on the assumption about Lipschitz Continuous, we can obtain: $|\mathcal{L}(\theta_{t+1}) - \mathcal{L}(\theta_t) - \langle \nabla \mathcal{L}(\theta_t), \theta_{t+1} - \theta_t \rangle| \leq \frac{L(l)}{2} \|\theta_{t+1} - \theta_t\|^2$.

Then, we can obtain:

$$\mathcal{L}_{\hat{z}}(\theta_{t+1}) - \mathcal{L}_{\hat{z}}(\theta_t) - \langle \widehat{\nabla} \mathcal{L}_{\hat{z}}(\theta_t), \theta_{t+1} - \theta_t \rangle \leq |\mathcal{L}_{\hat{z}}(\theta_{t+1}) - \mathcal{L}_{\hat{z}}(\theta_t) - \langle \widehat{\nabla} \mathcal{L}_{\hat{z}}(\theta_t), \theta_{t+1} - \theta_t \rangle| \leq \frac{L(l)}{2} \|\theta_{t+1} - \theta_t\|^2 \tag{22}$$

Based on the equation, we can follow the update rule: $\theta_{t+1} = \theta_t - \eta_t g_{\hat{z}}(\theta_t)$ and we can find:

$$\begin{aligned}
 \mathcal{L}_{\hat{z}}(\theta_{t+1}) &\leq \mathcal{L}_{\hat{z}}(\theta_t) + \langle \widehat{\nabla} \mathcal{L}_{\hat{z}}(\theta_t), \theta_{t+1} - \theta_t \rangle + \frac{L(l)}{2} \|\theta_t - \theta_{t+1}\|^2 \\
 &= \mathcal{L}_{\hat{z}}(\theta_t) - \eta_t \langle \widehat{\nabla} \mathcal{L}_{\hat{z}}(\theta_t), g_{\hat{z}}(\theta_t) \rangle + \frac{(\eta_t)^2 L(l)}{2} \|g_{\hat{z}}(\theta_t)\|^2
 \end{aligned} \tag{23}$$

where η_t represents the learning rate at step t . Then, we can take the expectation of Equation 23 for \hat{z} and input x :

$$\begin{aligned}
 & \mathbb{E}_{\hat{z},x}[\mathcal{L}_{\hat{z}}(\theta_{t+1})] \\
 & \leq \mathbb{E}_{\hat{z},x}[\mathcal{L}_{\hat{z}}(\theta_t)] - \eta_t \mathbb{E}_{\hat{z},x}[\|\widehat{\nabla} \mathcal{L}_{\hat{z}}(\theta_t)\|^2] + \frac{(\eta_t)^2 L(l_z)}{2} \mathbb{E}_{\hat{z},x}[\|g_z(\theta_t)\|^2] \\
 & \leq \mathbb{E}_{\hat{z},x}[\mathcal{L}_{\hat{z}}(\theta_t)] - \eta_t \mathbb{E}_{\hat{z},x}[\|\widehat{\nabla} \mathcal{L}_{\hat{z}}(\theta_t)\|^2] + \frac{(\eta_t)^2 L(l)}{2} (4(\hat{d}_t + 4) \mathbb{E}_{\hat{z},x}[\|\widehat{\nabla} \mathcal{L}_{\hat{z}}(\theta_t)\|^2] + 3\epsilon^2 L^2(l)(\hat{d}_t + 4)^3)
 \end{aligned} \tag{24}$$

The first inequality is due to the Equation 9 and Equation 23. The second inequality holds because Equation 21 provides the result about $\mathbb{E}_{\hat{z},x}[\|g_z(\theta_t)\|^2]$.

Then, we can select learning rate $\eta_t = \frac{1}{4(\hat{d}_t + 4)L(l)}$ and obtain:

$$\mathbb{E}_{\hat{z},x}[\mathcal{L}_{\hat{z}}(\theta_{t+1})] \leq \mathbb{E}_{\hat{z},x}[\mathcal{L}_{\hat{z}}(\theta_t)] - \frac{1}{8(\hat{d}_t + 4)L(l)} \mathbb{E}_{\hat{z},x}[\|\widehat{\nabla} \mathcal{L}_{\hat{z}}(\theta_t)\|^2] + \frac{3\epsilon^2}{32} L(l)(\hat{d}_t + 4) \tag{25}$$

Then, taking the sum of Equation 25 over the index from $T + 1$ to 0, we can have that :

$$\mathbb{E}_{\hat{z},x}[\|\widehat{\nabla} \mathcal{L}_{\hat{z}}(\theta_T)\|^2] \leq 8(\hat{d} + 4)L \left[\frac{\mathcal{L}_{\hat{z}}(\theta_0) - \mathcal{L}_{\hat{z}}^*}{T + 1} + \frac{3\epsilon^2}{32} L(\hat{d} + 4) \right] \tag{26}$$

where $L(l) \leq L$ for all $\mathcal{L}(\theta_t)$. Thus, based on Lemma 3.3, we can have:

$$\begin{aligned}
 \mathbb{E}_{\hat{z},x}[\|\nabla \mathcal{L}_m(\theta_T)\|^2] & \leq \frac{\epsilon^2 L^2}{2} (\hat{d} + 4)^3 + 2\mathbb{E}_{\hat{z},x}[\|\widehat{\nabla} \mathcal{L}_{\hat{z}}(\theta_T)\|^2] \\
 & \leq 16(\hat{d} + 4)L \frac{\mathcal{L}_{\hat{z}}(\theta_0) - \mathcal{L}_{\hat{z}}^*}{T + 1} + \frac{\epsilon^2 L^2}{2} (\hat{d} + 4)^2 (\hat{d} + \frac{11}{2})
 \end{aligned} \tag{27}$$

The second inequality is due to the Equation 26. To obtain σ -accurate solution: $\mathbb{E}_{\hat{z},x}[\|\nabla \mathcal{L}_m(\theta_T)\|^2] \leq \sigma^2$, we can define $\epsilon = \Omega(\frac{\sigma}{\hat{d}^{\frac{3}{2}} L})$.

$$\begin{aligned}
 16(\hat{d} + 4)L \frac{\mathcal{L}_{\hat{z}}(\theta_0) - \mathcal{L}_{\hat{z}}^*}{T + 1} + \mathcal{O}(\epsilon^2 L^2 \hat{d}^3) & = 16(\hat{d} + 4)L \frac{\mathcal{L}_{\hat{z}}(\theta_0) - \mathcal{L}_{\hat{z}}^*}{T + 1} + \mathcal{O}(\sigma^2) \\
 T & = \mathcal{O}\left(\frac{\hat{d}L}{\sigma^2}\right)
 \end{aligned} \tag{28}$$

Finally, we can finish the proof of the theorem. This theorem illustrates that the presence of pronounced sparsity patterns, along with the smoothness of the objective function, can significantly enhance the rate of convergence, potentially achieving a linear acceleration.